

Article

Not peer-reviewed version

Alterations in Rat Hippocampal Glutamatergic System Properties After Prolonged Febrile Seizures

Alexandra V. Griflyuk , [Tatyana Y. Postnikova](#) , [Sergey L. Malkin](#) , [Aleksy V. Zaitsev](#) *

Posted Date: 6 November 2023

doi: 10.20944/preprints202311.0289.v1

Keywords: febrile seizures; hypertherippocampmia; hus; maximal electroshock seizure threshold test; epilepsy; local field potential



Preprints.org is a free multidiscipline platform providing preprint service that is dedicated to making early versions of research outputs permanently available and citable. Preprints posted at Preprints.org appear in Web of Science, Crossref, Google Scholar, Scilit, Europe PMC.

Copyright: This is an open access article distributed under the Creative Commons Attribution License which permits unrestricted use, distribution, and reproduction in any medium, provided the original work is properly cited.

Article

Alterations in Rat Hippocampal Glutamatergic System Properties after Prolonged Febrile Seizures

Alexandra V. Griflyuk, Tatyana Y. Postnikova, Sergey L. Malkin and Aleksey V. Zaitsev *

Sechenov Institute of Evolutionary Physiology and Biochemistry of RAS, 44, Toreza Prospekt, Saint Petersburg 194223, Russia; griflyuk.al@mail.ru (A.G); tapost2@mail.ru (T. P.);

* Correspondence: aleksey_zaitsev@mail.ru

Abstract: Febrile seizures in early childhood can lead to developmental disorders in the CNS. However, the specific mechanisms behind the impact of febrile seizures on the developing brain are not well-understood. To address this gap in knowledge, we employed a hyperthermic model of febrile seizures in 10-day-old rats and tracked their development over two months. Our objective was to determine the degree to which the properties of the hippocampal glutamatergic system are modified. We analyzed whether pyramidal glutamatergic neurons in the hippocampus die after febrile seizures. Our findings indicate that there is a reduction in the number of neurons in various regions of the hippocampus in the first two days after seizures. The CA1 field showed the greatest susceptibility, and the reduction in the number of neurons in post-FS rats in this area appeared to be long-lasting. Electrophysiological studies indicate that febrile seizures cause a reduction in glutamatergic transmission, leading to decreased local field potential amplitude. This impairment could be attributable to diminished glutamate release probability as evidenced by decreases in frequency of miniature excitatory postsynaptic currents and increases in pair-pulse ratio of synaptic responses. We also found higher threshold current causing hindlimb extension in the maximal electroshock seizure threshold test of rats 2 months after febrile seizures compared to control animals. Our research suggests that febrile seizures can impair glutamatergic transmission, which may protect against future seizures.

Keywords: febrile seizures; hyperthermia; hippocampus; maximal electroshock seizure threshold test; epilepsy; local field potential

1. Introduction

Febrile seizures are the most common type of seizures in childhood, with a prevalence rate of 2–5% among children aged 6 months to 5 years [1]. Febrile seizures can be classified as simple or complex, depending on the duration and recurrence of episodes. Simple seizures typically last less than 15 minutes and occur no more than once a day. About 70% of all reported cases of childhood seizures are simple seizures. Complex seizures are defined as seizures that last longer than 15 minutes or involve repeated episodes over a 24-hour period. The most severe form of complex febrile seizures is febrile status epilepticus, which involves seizures lasting more than 30 minutes [2]. The relationship between febrile seizures and the development of temporal lobe epilepsy is uncertain. However, cohort studies indicate that children with complex febrile seizures have a significantly higher risk of developing temporal lobe epilepsy than those with simple febrile seizures [3–5].

To understand the mechanisms underlying potential epileptogenesis after febrile seizures, animal models must replicate the basic features of such seizures in children, including age and body temperature at onset. In this study, we utilized a well-established model of febrile seizures [6] that enabled tight control over seizure duration, thereby facilitating accurate modeling of the complex form of febrile seizures.

Several mechanisms are thought to cause epileptogenesis after complex febrile seizures. In particular, limbic seizures in the mature brain can result in the loss of vulnerable cells in the hippocampus, which may contribute to the development of epilepsy. Febrile seizures primarily occur in early childhood when the nervous system is still developing. Whether febrile seizures cause neuronal death remains a topic of debate. Clinical cases have described hippocampal edema in

children within 48 hours of prolonged febrile seizures, which resolves within 5 days [7]. Studies on animal models of febrile seizures indicate that there is no significant death of hippocampal neurons, but they do indicate cell damage and mossy fiber overgrowth [8,9]. As part of this study, we evaluated the incidence of neuronal death in the rat hippocampus at varying intervals following prolonged febrile seizures to examine the short- and long-term effects of these seizures on hippocampal morphology.

Neuroinflammation may accompany febrile seizure development and epileptogenesis. Studies have revealed increased levels of pro-inflammatory cytokines in the serum of children who experienced febrile seizures [10,11] and in animal models of febrile seizures [12]. This can result in chronic hyperexcitability of neuronal circuits and epilepsy development [13]. However, it remains unclear whether there is an increase in neuronal excitability after febrile seizures. One study shows a reduction in the amplitude of population spikes in CA1 field neurons when Schaffer collaterals are stimulated, as a result of enhanced inhibitory postsynaptic currents in the rat hippocampus one week after febrile seizures [14]. However, when Schaffer collaterals are stimulated with a series of stimuli, epileptiform activity develops only in slices obtained from animals after febrile seizures compared to controls, indicating increased excitability of hippocampal neuronal circuits [15]. Our study focused on examining excitatory synaptic transmission in the hippocampus of animals at different time points after febrile seizures to assess acute and long-term changes. In addition, we assessed the seizure threshold of the animals *in vivo* two months post febrile seizures.

2. Results

2.1. Febrile Seizures Provokes Neuronal Loss in the CA1 Region of the Rat Hippocampus

Whether febrile seizures induce loss of hippocampal neurons remains a topic of controversy, with conflicting data from clinical studies and animal experiments [8,9,16,17]. To assess the effect of prolonged febrile seizures at P10 on neuronal damage in rats, we used Nissl staining on brain slices and determined the number of neurons in different areas of the hippocampus, including CA1, CA3, hilus, and dentate gyrus, at different ages (P12, P21, and P55) (Figures 1 and 2). A two-way ANOVA revealed a significant effect of febrile seizures, age and their interaction on neuron number only in the hippocampal CA1 region (Figure 2A; $F(\text{FS})_{1,41} = 101.7$; $p < 0.0001$; $F(\text{Age})_{2,41} = 110.8$; $p < 0.0001$; $F(\text{FS} \times \text{Age})_{2,41} = 4.8$; $p < 0.01$). Tukey's post hoc tests revealed significant differences in the number of neurons both between control animals and animals after febrile seizures (post-FS rats) at different ages, and a decrease in neurons during development (P12: control: 62.1 ± 1.1 neurons per $100 \mu\text{m}$, post-FS: 52.1 ± 1.0 ; P21: control: 51.2 ± 1.0 , post-FS: 46.8 ± 1.0 ; P55: control: 47.6 ± 0.4 , post-FS: 40.1 ± 0.6).

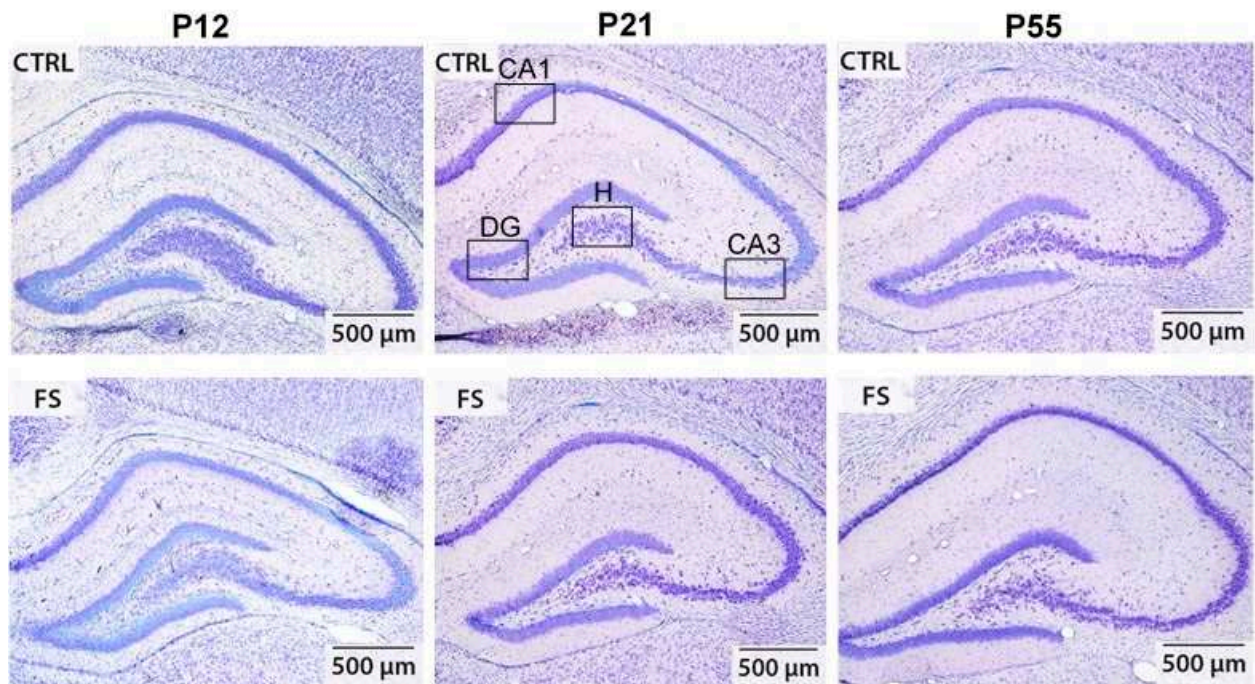


Figure 1. Representative images (50× magnification) show Nissl-stained, 20 μm-thick frontal sections of the hippocampus in control (CTRL) and experimental post-FS (FS) rats of varying ages. The black boxes highlight the regions where neuron quantification was conducted, including CA1, CA3, hilus (H), and dentate gyrus (DG).

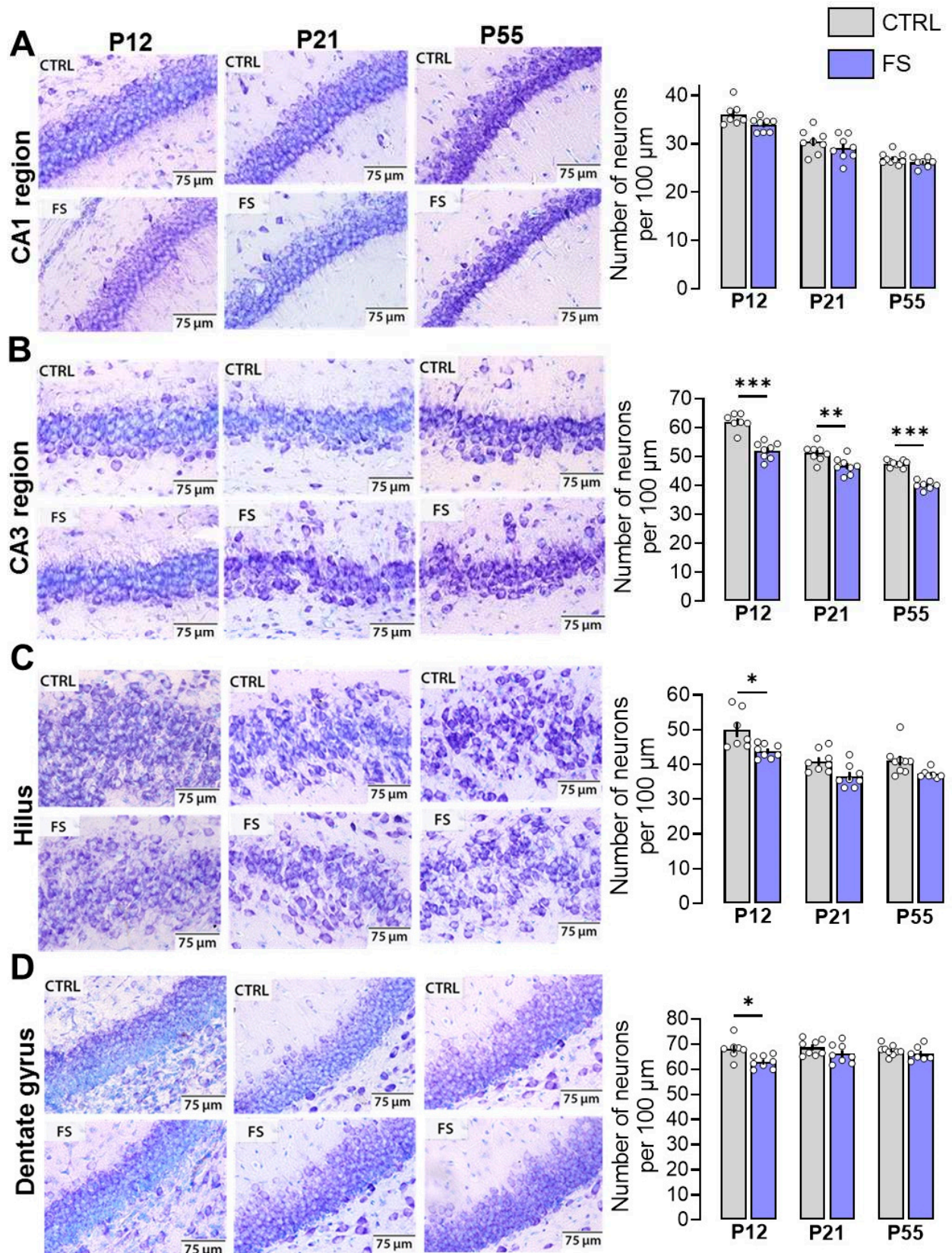


Figure 2. Nissl staining of neurons in hippocampal areas CA1 (A), CA3 (B), hilus (C) and dentate gyrus (D) in control (CTRL) and experimental post-FS (FS) rats. Diagrams showing the number of Nissl stained neurons per 100 μm cell layer. The circles show the individual values for each rat. Asterisks indicate significant differences between groups according to Tukey's post hoc test: * $p < 0.05$, ** $p < 0.01$, *** $p < 0.001$. Only between-group differences are presented.

In the in the hippocampal CA3 region and hilus, a two-way ANOVA revealed significant effects of age and febrile seizures, but there was no interaction of the factors (Figure 2B; CA3 region: $F(\text{FS})_{1,41} = 6.7$; $p < 0.05$; $F(\text{Age})_{2,41} = 75.5$; $p < 0.0001$; $F(\text{FS} \times \text{Age})_{2,41} = 0.5$; $p = 0.60$. Figure 2C; Hilus: $F(\text{FS})_{1,41} = 21.9$; $p < 0.0001$; $F(\text{Age})_{2,41} = 26.6$; $p < 0.0001$; $F(\text{FS} \times \text{Age})_{2,41} = 0.5$; $p = 0.64$). In the CA3 area, Tukey's post hoc tests revealed a decrease in the number of neurons with increasing age in both the control and experimental groups (P12: control: 36.2 ± 0.9 neurons per $100 \mu\text{m}$, post-FS: 33.9 ± 0.5 ; P21: control: 30.4 ± 0.9 , post-FS: 29.1 ± 0.9 ; P55: control: 26.9 ± 0.4 , post-FS: 26.2 ± 0.4). In hilus, in addition to age-related changes, there is a decrease in the number of neurons in animals after febrile seizures at P12 (P12: control: 49.9 ± 2.1 neurons per $100 \mu\text{m}$, post-FS: 43.8 ± 0.7 ; P21: control: 40.9 ± 1.1 , post-FS: 36.6 ± 1.1 ; P55: control: 41.1 ± 1.4 , post-FS: 37.2 ± 0.5).

In the dentate gyrus, only the effect of febrile seizures was revealed (Figure 2D; $F(\text{FS})_{1,41} = 10.9$; $p < 0.01$; $F(\text{Age})_{2,41} = 1.4$; $p = 0.25$; $F(\text{FS} \times \text{Age})_{2,41} = 1.5$; $p = 0.23$). Tukey's post hoc tests revealed a reduction in the number of neurons in animals after febrile seizures compared to the control group only at P12 (P12: control: 68.1 ± 1.5 neurons per $100 \mu\text{m}$, post-FS: 62.9 ± 0.9 ; P21: control: 68.6 ± 1.1 , post-FS: 66.1 ± 1.4 ; P55: control: 67.4 ± 0.7 , post-FS: 66.1 ± 1.1).

We have shown that febrile seizures lead to a reduction in the number of neurons in different areas of the hippocampus. However, the CA1 field displayed the greatest susceptibility, with a decrease in the number of neurons in post-FS animals across all three age groups. A decrease in the number of neurons was only observed at P12 in the hilus and dentate gyrus. There were no changes related to febrile seizures in the CA3 region.

2.2. Synaptic Neurotransmission in the Hippocampus Changed after Febrile Seizures

To evaluate the basic synaptic neurotransmission at the CA3-CA1 pyramidal neuron synapses in hippocampal slices, afferent fibers underwent electrical stimulation with different current intensities (25–300 mA). The synaptic neurotransmission was evaluated in both post-FS animals and control animals across different ages (P12, P21-23, P51-55; Figure 3). The fiber volley (FV) amplitude, reflecting the number of CA3 axons that evoke action potentials, and the fEPSPs amplitude, reflecting the sum of excitatory postsynaptic responses occurring in the dendrites of CA1 pyramidal neurons in response to afferent fiber stimulation, were both recorded in each slice.

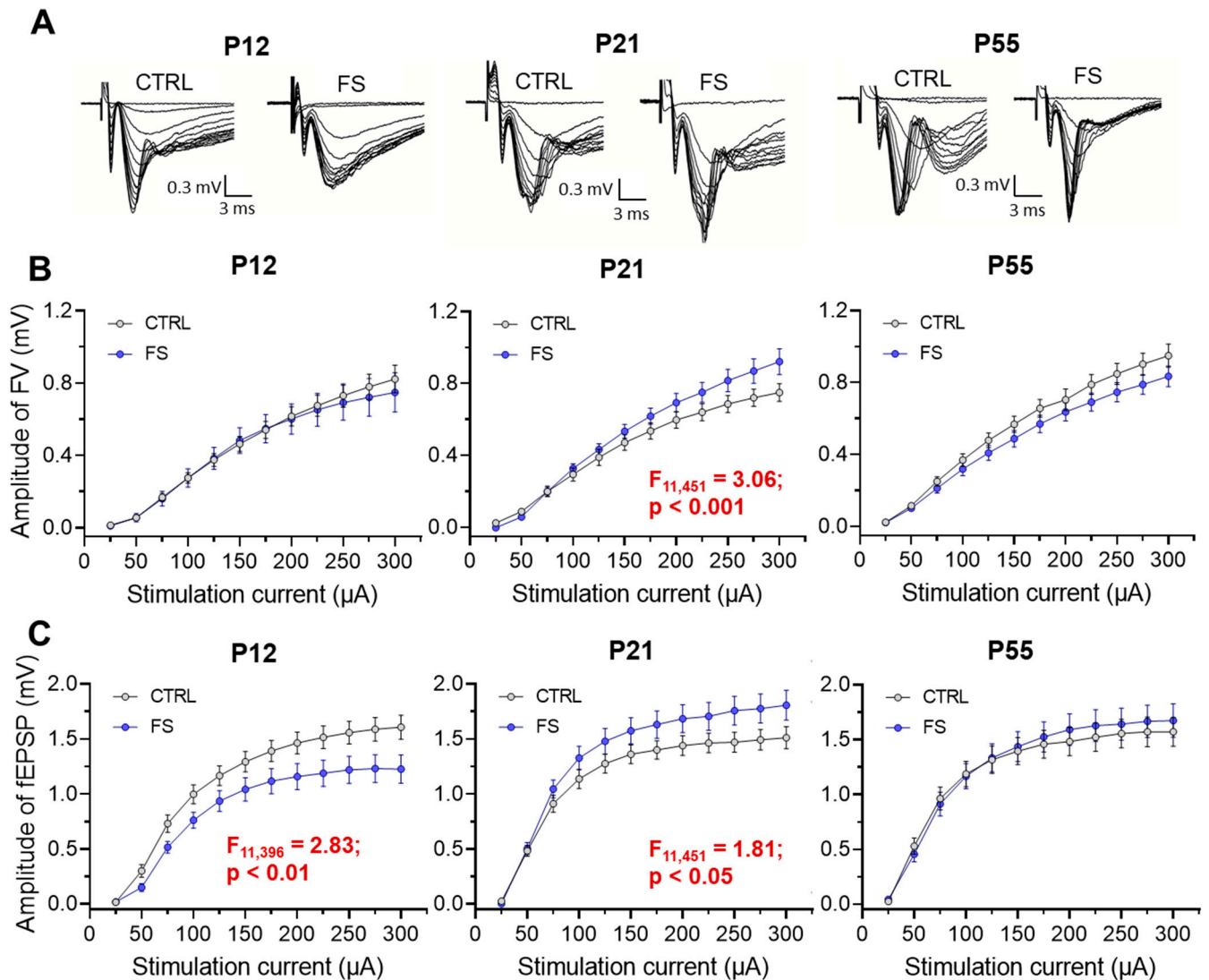


Figure 3. Synaptic neurotransmission in the hippocampus changed after febrile seizures. (A) Representative examples of fEPSPs recorded at different strengths of extracellular stimulation in the control (CTRL) and after febrile seizures animals (FS) of different ages (P12, P21, P55). Stimulation response relationships for presynaptic fiber volley (FV) amplitude (B) and fEPSP amplitudes (C) recorded from the hippocampal CA1 region. Data shown as means \pm standard errors of the means.

At P12 in post-FS animals, the fEPSP amplitude was reduced compared to the control ($F_{11,396} = 2.83$; $p < 0.01$, control: $n = 21$ slices; post-FS: $n = 17$), while no changes in the FV amplitude were observed ($F_{11,396} = 0.32$; $p = 0.98$). Conversely, at P21, an increase in the amplitudes of both FV ($F_{11,451} = 3.06$; $p < 0.001$, control: $n = 16$; post-FS: $n = 27$) and fEPSP ($F_{11,451} = 1.81$; $p < 0.05$) was observed in post-FS animals. At the age of 51–55 days, no statistically significant differences in these parameters were found between control animals and post-FS animals (amplitudes of FV: $F_{11,440} = 1.31$; $p = 0.21$, control: $n = 16$; post-FS: $n = 24$ and amplitudes of fEPSP: $F_{11,440} = 0.63$; $p = 0.80$).

2.3. Short-Term Synaptic Plasticity of Hippocampal Neurons Changes in Rats Two Days after febrile seizures

The decrease in fEPSP amplitude without a change in FV amplitude in rats two days after febrile seizures may be related to changes in the probability of glutamate release in Schaffer collaterals. To assess possible changes in the probability of mediator release after febrile seizures, we assessed short-term synaptic plasticity (STP) in rats of different ages [18]. To do this, we used a paired-pulse stimulation with an interstimulus interval of 10 to 500 ms and compared paired-pulse ratio (PPR) at

different intervals in control animals (P12: $n = 8$ slices; P21: $n = 12$; P55: $n = 9$) and post-FS animals (P12: $n = 8$; P21: $n = 15$; P55: $n = 9$). Repeated measures ANOVA revealed significant changes in PPR only in animals two days after febrile seizures, whereas no differences with the control group were found in animals at P21 and P55 (P12: $F_{14,196} = 3.22$; $p < 0.001$; P21: $F_{14,336} = 0.26$; $p = 0.99$; P55: $F_{14,224} = 0.12$; $p = 0.99$; Figure 4).

This experiment shows a decrease in the probability of mediator release in hippocampal CA3-CA1 synapses two days after febrile seizures. Later, however, these changes are no longer observed.

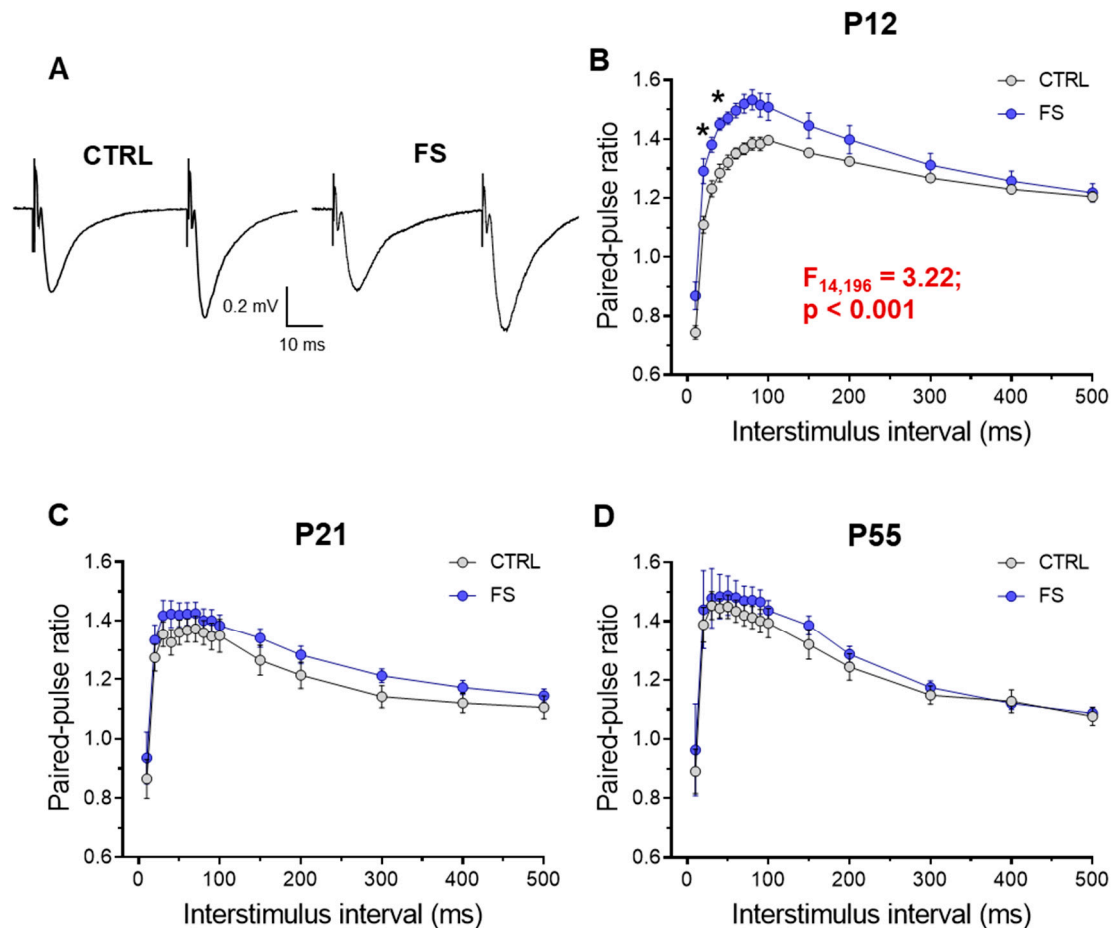


Figure 4. Paired-pulse facilitation altered in hippocampal slices 2 days after febrile seizures. (A) Representative examples of paired-pulse responses from the hippocampal in control rats (CTRL) and rats after febrile seizures (FS) at P12 using interstimulus intervals of 40 ms. (B-D) Diagrams of paired-pulse facilitation in rat hippocampal slices at P12 (B), P21-23 (C) days and P51-55 (D) at different interstimulus intervals. Asterisks indicate significant differences according to Tukey's post hoc test: * $p < 0.05$.

2.4. Frequency of Miniature Excitatory Postsynaptic Current is Reduced Two Days after Febrile Seizures

Since we observed significant changes in synaptic transmission in rats 2 days after experiencing febrile seizures, we analyzed the properties of miniature excitatory postsynaptic currents (mEPSC) in CA1 neurons, including their amplitudes, kinetics, and frequency in control and post-FS groups recorded at -80 mV.

Our findings indicate that the frequency of mEPSCs decreased by 47% (Control: 0.67 ± 0.06 Hz; $n = 20$, post-FS: 0.42 ± 0.02 Hz, $n = 21$, $p < 0.001$). Meanwhile, the other mEPSC parameters, including amplitude (control: 18.4 ± 1.1 pA, $n = 17$, post-FS: 17.7 ± 1.2 pA, $n = 22$, $p = 0.66$), rise time (control: 1.52 ± 0.19 ms, $n = 20$, post-FS: 1.37 ± 0.11 ms, $n = 24$, $p = 0.46$), and decay time constant (control: 5.32 ± 0.39 ms, $n = 19$, post-FS: 4.42 ± 0.32 ms, $n = 21$, $p = 0.14$), remained unaltered (Figure 5).

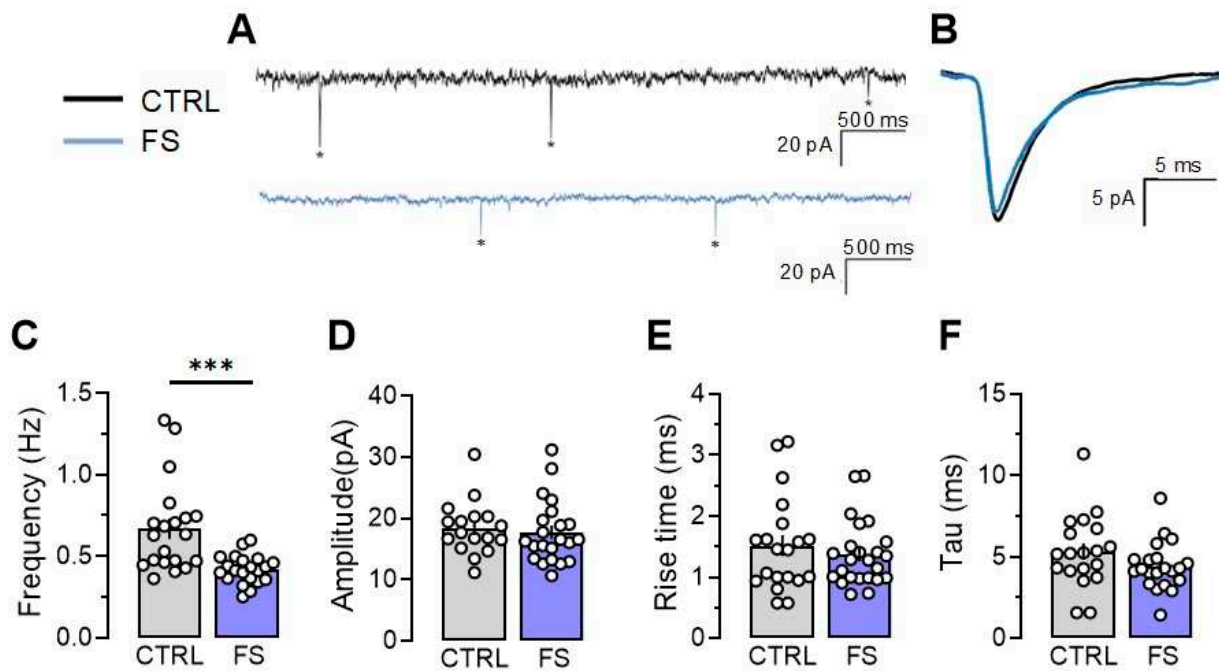


Figure 5. Frequency of miniature excitatory postsynaptic current (mEPSC) is reduced two days after experiencing febrile seizures. (A) Representative current responses from CA1 pyramidal neurons recorded at -80 mV and (B) examples of averaged mEPSCs in control (CTRL) and post-FS (FS) animals. The frequency (C), amplitude (D), rise time (E), and decay time constant (F) of mEPSC in the control and post-FS groups are presented. Asterisks indicate significant differences between groups according to Student's test: *** $p < 0.001$.

This suggests that presynaptic mechanisms likely trigger changes in synaptic strength in CA1 neurons. Consequently, our research shows that febrile seizures can result in impaired glutamatergic transmission during the first few days following a seizure, which might serve as a protective factor in reducing the possibility of future seizures.

2.5. Rats after Febrile Seizures Have an Increased Threshold for Maximal Electroshock Seizure

Since prolonged febrile seizures in early childhood may increase the risk of developing epilepsy, it was hypothesized that the threshold for seizure onset would be reduced in post-FS rats. To evaluate this hypothesis, the maximal electroshock seizure threshold (MEST) test was conducted on rats 2 months after febrile seizures ($n = 14$) and on control animals of the same age ($n = 17$). The results showed that post-FS rats had a significantly higher threshold for tonic hind limb extension ($U_{17,14} = 27$, $p < 0.001$, Figure 6).

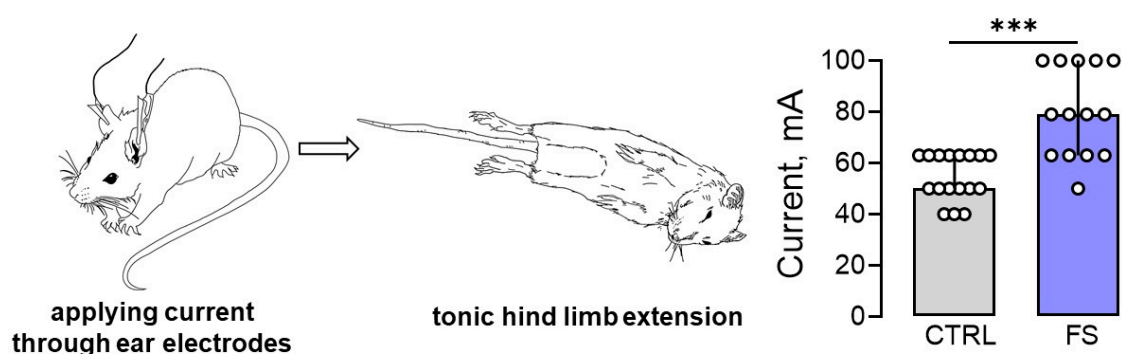


Figure 6. The maximal electroshock seizure threshold (MEST) increased in rats 2 months after febrile seizures. Image of a rat with tonic hind limb extension induced by applying current through ear

electrodes. Diagrams illustrating the differences in threshold currents in the control (CTRL) and post-FS (FS) animals required for tonic hind limb extension. The circles show the individual values for each rat. Asterisks indicate significant differences between groups according to Mann-Whitney U test: *** $p < 0.001$. Data are represented as median with interquartile range.

Thus, our experimental model of febrile seizures revealed a surprising outcome: early childhood febrile seizures may actually raise the threshold for tonic seizure generation, rather than lower it as previously believed.

3. Discussion

Febrile seizures are the most common type of seizure in young children [2,19,20]. However, the association of febrile seizures with subsequent hippocampal damage and the development of temporal lobe epilepsy remains undetermined. A retrospective analysis of patients with temporal lobe epilepsy shows a high prevalence of febrile seizures in the history, which may suggest an etiological role of these seizures in the development of temporal lobe epilepsy [21,22]. However, according to population-based and prospective epidemiological studies, febrile seizures do not progress to temporal lobe epilepsy [23]. In this study, we aimed to investigate whether hippocampal neuronal death and changes in hippocampal excitability occur at different developmental ages after prolonged febrile seizures in early life.

We found that the CA1 region of the hippocampus showed the most significant loss of neurons. Furthermore, two days post-seizure, there was impaired glutamatergic transmission, with a lower probability of mediator release and a decline in baseline synaptic transmission at CA3-CA1 synapses. Interestingly, the baseline neurotransmission in rats increases at 3 weeks of age, 11 days after seizures. However, there were no alterations in baseline synaptic transmission found 40-45 days after seizures. Despite this, the threshold for developing tonic convulsions in animals was observed to have increased two months after febrile seizures in comparison to the control group.

In this study, we confirmed the widely held belief that seizures in the developing brain do not result in significant loss of neurons. Prior research has indicated that there is minimal neuronal death in the hippocampus 20 hours after febrile seizures [8], whereas there is no neuronal death in adult animals that have experienced febrile seizures during their early stages of life [8,9]. Our findings generally support these previous observations.

Four hippocampal regions were compared in this study across three animal age groups. After febrile seizures, the number of neurons decreased in the CA1 region, hilus, and dentate gyrus within two days - the earliest point of the study. Conversely, there was no loss of neurons in the CA3 region of the hippocampus. Nevertheless, after 10 days and 1.5 months, only the CA1 region displayed observable differences between post-FS and control groups. These findings are consistent with data from other immature animal seizure models (lithium-pilocarpine model of status epilepticus and kainic acid model of temporal lobe epilepsy), where hippocampal CA1 neurons have been shown to be more vulnerable than other hippocampal regions [24–26]. One possible explanation for why CA1 neurons in the hippocampus are more prone to febrile seizures at P10 is the delayed development of synaptic inhibition in CA1 compared to CA3 during early postnatal ontogeny [27]. It is worth mentioning that neurogenesis persists in the dentate gyrus during the postnatal period, potentially accounting for the absence of differences at later stages. Nonetheless, dentate gyrus cells generated after febrile seizures exhibit augmented spontaneous excitatory input [28].

We observed an age-related decrease in the number of neurons in the CA1 and CA3 regions, as well as in the hilus, both in the control group and in animals after febrile seizures. The number of neurons in the hilus does not differ from the control group by 21 days of age due to this process. However, differences persist in the CA1 region because neuronal death in this area was more pronounced in the early days after seizures.

Concurrently with examining morphological changes, we investigated the excitatory synaptic transmission in the CA3-CA1 neurons of the hippocampus. The most significant changes were observed two days after febrile seizures, with a reduction in synaptic transmission efficacy, changes

in short-term plasticity, and a decrease in the frequency of miniature excitatory synaptic currents. Overall, the findings indicate a decrease in the probability of mediator release in hippocampal CA3-CA1 synapses. These changes in the probability of glutamate release may shift the balance of excitation and inhibition toward inhibition and reduce the risk of seizure activity in hippocampal neuronal networks.

Opposite changes can occur in various models of seizures and epilepsy. For instance, in the 4-aminopyridine *in vitro* model, no changes were noticed in the frequency of mEPSCs and the paired amplitude ratio of evoked responses, one hour after epileptiform activity. However, potentiation of the synaptic transmission was observed due to postsynaptic changes [29]. Similarly, one hour after neonatal hypoxic seizures, researchers observed an increase in synaptic transmission attributed to increased mEPSC amplitude mediated by AMPA receptors [30]. Moreover, the authors of this study found that hypoxia-induced seizures resulted in an increased mEPSC frequency, indicating a combined pre- and postsynaptic potentiation [30]. The amplitude, but not the frequency, of mEPSCs recorded from CA1 pyramidal neurons was found to be increased in slices taken from animals with pilocarpine-induced status epilepticus [31]. In other study using lithium-pilocarpine model, the evoked EPSC amplitudes were increased 20-60 days after the pilocarpine seizures, and then decreased further into the chronic phase of the epilepsy model [32]. In the repeated low-dose kainate model of epilepsy, 1 week after the induction of seizures the increased mEPSC frequency was observed, although the amplitudes were similar to control [33].

In many models of seizures and epilepsy, synaptic potentiation results from the NMDA-dependent incorporation of AMPA receptors, which includes an increase in the proportion of calcium-permeable AMPA receptors [30,31,34–36]. Neuroinflammation can increase the proportion of calcium-permeable AMPA receptors. Specifically, administering bacterial lipopolysaccharide in experimental studies showed elevated GluA1 expression following LPS treatment in two-week-old [37,38] and two-month-old rats [39]. Conversely, febrile seizures cause a rapid decrease in the proportion of calcium-permeable AMPA receptors in the synapses of pyramidal neurons [40].

The difference may be due to the febrile seizure model used in our experiments, which does not lead to the development of chronic epilepsy in rats. Therefore, the synaptic changes rapidly disappear after the seizures since no epileptogenesis occurs. Nonetheless, in a comparable febrile seizure model, it was revealed that glutamate release probability increased two months following the seizure [28]. It should be noted, however, that these modifications were identified in dentate granule cells instead of the CA1 region.

Unexpectedly, we found a higher current threshold for the development of tonic seizures in *in vivo* experiments. However, previous studies have shown an increased susceptibility to seizures in adult rats at least three months after febrile seizures [15] and electroencephalographically recorded epileptiform discharges in the limbic system [41]. In contrast, a previous study found that young animals exhibited reduced susceptibility to pentylenetetrazole-induced seizures 20 days after experiencing febrile seizures [42]. These results are consistent with our own findings in animals observed 2 months after seizures. It is possible that the discrepancies in results are due to differences in the age of the animals evaluated for seizure susceptibility. It is possible that after febrile seizures, neural circuit excitability may be reduced in animals as a compensatory to reduce the risk of developing of recurrent seizures. Nevertheless, further research is necessary to support this hypothesis.

However, reducing excitatory transmission in the immature brain could potentially delay its further development. This is because the maturation and morphological changes of astrocytes rely on neuronal activity, and astrocytes regulate synaptogenesis in the immature brain [43,44]. This could hamper the maturation of synaptic plasticity processes, leading to potential cognitive impairment, as previously demonstrated [45].

4. Materials and Methods

4.1. Animals

Wistar rats were utilized in this study. Animals were housed in standard conditions with unrestricted access to food and water. The Ethics Committee of the Sechenov Institute of Evolutionary Physiology and Biochemistry approved all experiments and ensured compliance with local guidelines for laboratory animal welfare. These conditions fully comply with international regulations for animal experimentation. The sequence of experiments performed is shown in the scheme (Figure 7).

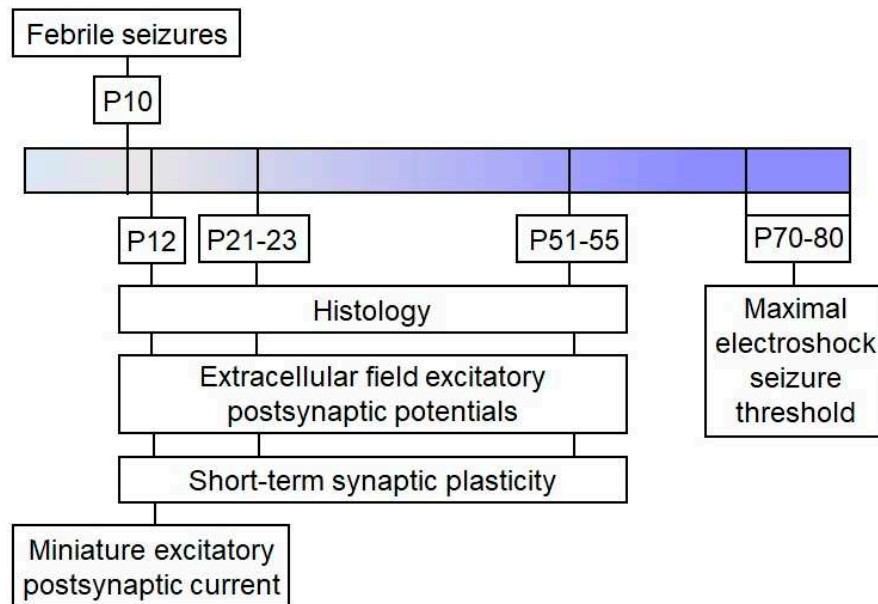


Figure 7. The experimental design.

4.2. Febrile Seizures Model

Febrile seizures were induced on postnatal day 10 as described previously [6,45]. Briefly, P10 pups were placed at the bottom of a glass chamber for 30 minutes and exposed to a regulated stream of heated air, keeping the chamber temperature at 46 °C. Most animals had their body temperature rise to 39 °C within the first 10 minutes under these conditions, and often showed facial automatisms, sometimes accompanied by unilateral body flexion. This was followed by myoclonic twitching of the hind limbs, followed by clonic convulsions. Rectal body temperature was measured every two minutes and maintained below 41 °C during episodes of convulsions. The study included a total of 63 animals with FS durations of at least 15 minutes. After hyperthermia, the pups were placed on a cold surface until their core temperature was normalized, and then returned to their nest. The littermates utilized as controls were removed from the nest for the same duration but were kept at room temperature (N=65).

4.3. Histology

At P12, P21–23, and P51–55, rats were anesthetized with a mixture of Zoletil (3 mg per 100 g) and xylazine (50 µL per 100 g) diluted in saline. Afterwards, the rats were perfused transcardially with phosphate-buffered saline (PBS, pH 7.4, 0.01 M), followed by 4% paraformaldehyde (PFA) in PBS. Subsequently, the animals were decapitated, the brain removed and fixed in 4% PFA at 4°C for at least 2 days. After fixation, brains were cryoprotected in 30% sucrose. Brains were frozen in cooled (<−50°C) isopentane (78-78-4, Isopentane Solution, Sigma-Aldrich, St. Louis, MO, USA) and stored at −80°C.

Serial 20- μm thick frontal sections were cut on a Bright OTF5000 cryostat (Bright Instrument Co Ltd, Huntingdon, UK) at -2.6 to -3.6 mm bregma, placed on Super Frost Plus-coated slides (J1800AMNZ, Fisher Scientific UK Ltd, Loughborough, UK), and air dried for 1 day. Nissl staining was performed as previously described in details [46]. Nissl-stained sections were analyzed using a Leica AF 7000 microscope (Leica Microsystems, Wetzlar, Germany) at $\times 400$ magnification. For morphological analysis, neurons were counted in 6–8 sections from one animal, with the distance between analyzed sections being 100 μm . The number of neurons in the micrographs was counted in the 100 μm region for the cell layers in CA1, CA3, hilus, and dentate gyrus using ImageJ 1.52a software (U.S. National Institutes of Health, Bethesda, MD, USA).

4.3. Brain Slice Preparation

At P12, P21-23, and P51-55, the rats were decapitated and their brains were quickly removed. Using an HM 650 V vibratome (Microm, Walldorf, Germany), horizontal brain slices (400 μm) were cut in chilled artificial cerebrospinal fluid (ACSF) at a temperature of 0 $^{\circ}\text{C}$. The ACSF contained 126 mM NaCl, 24 mM NaHCO_3 , 2.5 mM KCl, 2 mM CaCl_2 , 1.25 mM NaH_2PO_4 , 1 mM MgSO_4 , and 10 mM glucose and was aerated with carbogen (95% O_2 and 5% CO_2). Afterward, the slices were allowed to recover for 1 hour at 35 $^{\circ}\text{C}$ in oxygenated ACSF.

4.4. Field Potential Recordings

Field potentials were recorded in the CA1 stratum radiatum of the hippocampus using glass microelectrodes (0.2-1.0 $\text{M}\Omega$), following the procedures outlined in previous studies [47,48]. Each slice was stimulated with increasing amplitude currents (25 to 300 μA , 25 μA increments) to measure fEPSP and FV amplitudes. Paired pulses with varying interstimulus intervals were administered every 20 s to ascertain the paired-pulse ratio (PPR), calculated as the amplitude ratio between the first fEPSP and the second. Intervals ranged from 10 to 500 ms.

4.5. Patch-Clamp Recordings

The recordings were performed at 30 $^{\circ}\text{C}$. Neurons in the pyramidal layer of the CA1 hippocampus were visualized using a Zeiss Axioskop 2 microscope (Zeiss, Oberkochen, Germany) equipped with differential interference contrast optics and a video camera (Sanyo VCB-3512P, Sanyo Electric, Osaka, Japan). Patch electrodes with resistance of 2-4 $\text{M}\Omega$ were fabricated from borosilicate glass capillaries (Sutter Instrument, Novato, CA, USA) using a P-1000 Micropipette Puller (Sutter Instrument). For recording miniature excitatory synaptic currents (mEPSCs), we employed a solution based on potassium gluconate. The solution's composition in mM was as follows: 114 K-gluconate, 6 KCl, 0.2 EGTA, 10 HEPES, 4 ATP-Mg, and 0.3 GTP. The pH level was adjusted to 7.25 using KOH.

Signals were recorded using a Multiclamp 700B patch-clamp amplifier (Molecular Devices, Sunnyvale, CA), InstruTECH LIH 8+8 ADC/DAC module (HEKA, Stuttgart, Germany), and WinWCP 5 software (University of Strathclyde, Glasgow, UK). The data underwent 3 kHz filtering and 16.67 kHz sampling. The access resistance was less than 20 $\text{M}\Omega$ for all whole-cell recordings included in the sample and remained stable ($\leq 20\%$ increase) across the experiments. No series resistance compensation was utilized during the experiment.

The mEPSC recordings were conducted at a membrane potential of -70 mV in the presence of 0.5 μM TTX (Alomone Labs, Jerusalem, Israel). The mEPSCs were detected offline with Clampfit 10.0 software (Molecular Devices) and their characteristics were analyzed utilizing software based on open-source SciPy and NumPy libraries for the Python programming language (Python Software Foundation, Wilmington, DE, USA).

4.6. Maximal electroshock seizure threshold (MEST)

To evaluate susceptibility to seizures in animals, we measured the MEST two months following febrile seizures. Current was applied via ear electrodes using an ECT Unit 57800 pulse generator (Ugo Basile, Italy), using stimulation currents ranging from 12 to 100 mA with log scale intervals of 0.1.

The pulse frequency was set at 150 Hz, pulse duration at 0.8 s, and pulse width at 0.9 ms. We determined the minimum current necessary to observe tonic hind limb extension for each animal. On day one, the animal received a current of 40 mA. If tonic hind limb extension was not observed, the current was increased by 1 step. If tonic hind limb extension occurred at 40 milliamperes, the current was decreased by 1 step. The tests were repeated every 2-3 days.

4.7. Statistical Analysis

Statistical analysis was conducted with Statistica 8.0 (Systat Software, Inc., Palo Alto, CA) and GraphPad Prism 8 software (GraphPad Software, San Diego, CA). We identified outliers using Dixon's Q-test and tested for normal distribution using the Kolmogorov-Smirnov test. We used Student's test, two-way ANOVA, or repeated-measures ANOVA as appropriate to assess statistical significance, followed by the Tukey's post hoc test, as described in the text. Statistical analysis of MEST test data was conducted using the Mann-Whitney U test. Results were presented as mean \pm standard error of the mean for normal distribution or median and interquartile range for non-normal distribution. A p-value less than 0.05 was considered statistically significant.

Author Contributions: Formal analysis, Tatyana Postnikova, Alexandra Griflyuk, and Sergey Malkin; Funding acquisition, Tatyana Postnikova; Investigation, Tatyana Postnikova, Alexandra Griflyuk, and Sergey Malkin; Methodology, Tatyana Postnikova; Supervision, Tatyana Postnikova and Aleksey Zaitsev; Validation, Tatyana Postnikova and Aleksey Zaitsev; Writing – original draft, Tatyana Postnikova, Alexandra Griflyuk, Sergey L. Malkin, and Aleksey Zaitsev; Writing – review & editing, Tatyana Postnikova, Alexandra Griflyuk, and Aleksey Zaitsev.

Funding: This research was funded by the Russian Science Foundation, grant number 23-25-00143.

Institutional Review Board Statement: "The study was conducted according to the EU Directive 2010/63/EU for animal experiments and approved by the Ethics Committee of the Sechenov Institute of Evolutionary Physiology and Biochemistry of the Russian Academy of Sciences (Ethical permit number 13-k-a, 15 February 2018).

Data Availability Statement: The data presented in this study are available on request from the corresponding author.

Acknowledgments: Histology experiments were performed using the facilities of the Research Resource Centre for physiological, biochemical, and molecular-biological research of the Sechenov Institute of Evolutionary Physiology and Biochemistry of the Russian Academy of Sciences.

Conflicts of Interest: The authors declare no conflict of interest.

References

1. Waruiru, C.; Appleton, R. Febrile Seizures: An Update. *Arch Dis Child* **2004**, *89*, 751–756, doi:10.1136/adc.2003.028449.
2. Leung, A.K.; Hon, K.L.; Leung, T.N.H. Febrile Seizures: An Overview. *Drugs Context* **2018**, *7*, 1–12, doi:10.7573/dic.212536.
3. Nelson, K.B.; Ellenberg, J.H. Predictors of Epilepsy in Children Who Have Experienced Febrile Seizures. *New England Journal of Medicine* **1976**, *295*, 1029–1033, doi:10.1056/NEJM197611042951901.
4. Verity, C.M.; Golding, J. Risk of Epilepsy after Febrile Convulsions: A National Cohort Study. *BMJ* **1991**, *303*, 1373–1376, doi:10.1136/bmj.303.6814.1373.
5. Civan, A.B.; Ekici, A.; Havali, C.; Kiliç, N.; Bostanci, M. Evaluation of the Risk Factors for Recurrence and the Development of Epilepsy in Patients with Febrile Seizure. *Arq Neuropsiquiatr* **2022**, *80*, 779–785, doi:10.1055/s-0042-1755202.
6. Baram, T.Z.; Gerth, A.; Schultz, L. Febrile Seizures: An Appropriate-Aged Model Suitable for Long-Term Studies. *Brain Res Dev Brain Res* **1997**, *98*, 265–270, doi:10.1016/s0165-3806(96)00190-3.
7. Scott, R.C. Hippocampal Abnormalities after Prolonged Febrile Convulsion: A Longitudinal MRI Study. *Brain* **2003**, *126*, 2551–2557, doi:10.1093/brain/awg262.
8. Toth, Z.; Yan, X.-X.X.; Haftoglou, S.; Ribak, C.E.; Baram, T.Z. Seizure-Induced Neuronal Injury: Vulnerability to Febrile Seizures in an Immature Rat Model. *The Journal of Neuroscience* **1998**, *18*, 4285–4294, doi:10.1523/JNEUROSCI.18-11-04285.1998.

9. Bender, R.A.; Dubé, C.; Gonzalez-Vega, R.; Mina, E.W.; Baram, T.Z. Mossy Fiber Plasticity and Enhanced Hippocampal Excitability, without Hippocampal Cell Loss or Altered Neurogenesis, in an Animal Model of Prolonged Febrile Seizures. *Hippocampus* **2003**, *13*, 399–412, doi:10.1002/hipo.10089.
10. Tütüncüoğlu, S.; Kütükçüler, N.; Kepe, L.; Çoker, C.; Berdeli, A.; Tekgül, H. Proinflammatory Cytokines, Prostaglandins and Zinc in Febrile Convulsions. *Pediatrics International* **2001**, *43*, 235–239, doi:10.1046/j.1442-200x.2001.01389.x.
11. Al Morshedy, S.; Elsaadany, H.F.; Ibrahim, H.E.; Sherif, A.M.; Farghaly, M.A.A.; Allah, M.A.N.; Abouzeid, H.; Elashkar, S.S.A.; Hamed, M.E.; Fathy, M.M.; et al. Interleukin-1 β and Interleukin-1receptor Antagonist Polymorphisms in Egyptian Children with Febrile Seizures. *Medicine* **2017**, *96*, e6370, doi:10.1097/MD.0000000000006370.
12. Dubé, C.M.; Ravizza, T.; Hamamura, M.; Zha, Q.; Keebaugh, A.; Fok, K.; Andres, A.L.; Nalcioğlu, O.; Obenaus, A.; Vezzani, A.; et al. Epileptogenesis Provoked by Prolonged Experimental Febrile Seizures: Mechanisms and Biomarkers. *J Neurosci* **2010**, *30*, 7484–7494, doi:10.1523/JNEUROSCI.0551-10.2010.
13. Devinsky, O.; Vezzani, A.; Najjar, S.; De Lanerolle, N.C.; Rogawski, M.A. Glia and Epilepsy: Excitability and Inflammation. *Trends Neurosci* **2013**, *36*, 174–184, doi:10.1016/j.tins.2012.11.008.
14. Chen, K.; Baram, T.Z.; Soltesz, I. Febrile Seizures in the Developing Brain Result in Persistent Modification of Neuronal Excitability in Limbic Circuits. *Nat Med* **1999**, *5*, 888–894, doi:10.1038/11330.
15. Dube, C.; Chen, K.; Eghbal-Ahmadi, M.; Brunson, K.; Soltesz, I.; Baram, T.Z.; Eghbal-Ahmadi, M.; Brunson, K.; Soltesz, I.; Baram, T.Z.; et al. Prolonged Febrile Seizures in the Immature Rat Model Enhance Hippocampal Excitability Long Term. *Ann Neurol* **2000**, *47*, 336–344, doi:10.1002/1531-8249(200003)47:3<336::AID-ANA9>3.3.CO;2-N.
16. Scott, R.C.; King, M.D.; Gadian, D.G.; Neville, B.G.R.; Connelly, A. Hippocampal Abnormalities after Prolonged Febrile Convulsion: A Longitudinal MRI Study. *Brain* **2003**, *126*, 2551–2557, doi:10.1093/brain/awg262.
17. Tanabe, T.; Hara, K.; Shimakawa, S.; Fukui, M.; Tamai, H. Hippocampal Damage after Prolonged Febrile Seizure: One Case in a Consecutive Prospective Series. *Epilepsia* **2011**, *52*, 837–840, doi:10.1111/j.1528-1167.2010.02958.x.
18. Zucker, R.S.; Regehr, W.G. Short-Term Synaptic Plasticity. *Annu Rev Physiol* **2002**, *64*, 355–405, doi:10.1146/annurev.physiol.64.092501.114547.
19. Sugai, K. Current Management of Febrile Seizures in Japan: An Overview. *Brain Dev* **2010**, *32*, 64–70, doi:10.1016/j.braindev.2009.09.019.
20. Verity, C.M.; Butler, N.R.; Golding, J. Febrile Convulsions in a National Cohort Followed up from Birth. I—Prevalence and Recurrence in the First Five Years of Life. *Br Med J (Clin Res Ed)* **1985**, *290*, 1307–1310, doi:10.1136/bmj.290.6478.1307.
21. Cendes, F.; Andermann, F.; Dubeau, F.; Gloor, P.; Evans, A.; Jones-Gotman, M.; Olivier, A.; Andermann, E.; Robitaille, Y.; Lopes-Cendes, I. Early Childhood Prolonged Febrile Convulsions, Atrophy and Sclerosis of Mesial Structures, and Temporal Lobe Epilepsy: An MRI Volumetric Study. *Neurology* **1993**, *43*, 1083–1087, doi:10.1212/wnl.43.6.1083.
22. French, J.A.; Williamson, P.D.; Thadani, V.M.; Darcey, T.M.; Mattson, R.H.; Spencer, S.S.; Spencer, D.D. Characteristics of Medial Temporal Lobe Epilepsy: I. Results of History and Physical Examination. *Ann Neurol* **1993**, *34*, 774–780, doi:10.1002/ana.410340604.
23. Nelson, K.B.; Ellenberg, J.H. Predictors of Epilepsy in Children Who Have Experienced Febrile Seizures. *New England Journal of Medicine* **1976**, *295*, 1029–1033, doi:10.1056/nejm197611042951901.
24. Thompson, K.; Wasterlain, C. Lithium-Pilocarpine Status Epilepticus in the Immature Rabbit. *Developmental Brain Research* **1997**, *100*, 1–4, doi:10.1016/S0165-3806(96)00209-X.
25. Franck, J.E.; Schwartzkroin, P.A. Immature Rabbit Hippocampus Is Damaged by Systemic but Not Intraventricular Kainic Acid. *Developmental Brain Research* **1984**, *13*, 219–227, doi:10.1016/0165-3806(84)90156-1.
26. Sankar, R.; Shin, D.H.; Liu, H.; Mazarati, A.; Pereira de Vasconcelos, A.; Wasterlain, C.G. Patterns of Status Epilepticus-Induced Neuronal Injury during Development and Long-Term Consequences. *The Journal of Neuroscience* **1998**, *18*, 8382–8393, doi:10.1523/JNEUROSCI.18-20-08382.1998.
27. Swann, J.W.; Brady, R.J.; Martin, D.L. Postnatal Development of GABA-Mediated Synaptic Inhibition in Rat Hippocampus. *Neuroscience* **1989**, *28*, 551–561, doi:10.1016/0306-4522(89)90004-3.

28. Hoogland, G.; Raijmakers, M.; Clynen, E.; Brône, B.; Rigo, J.-M.; Swijsen, A. Experimental Early-Life Febrile Seizures Cause a Sustained Increase in Excitatory Neurotransmission in Newborn Dentate Granule Cells. *Brain Behav* **2022**, *12*, e2505, doi:10.1002/brb3.2505.
29. Ergina, J.L.; Amakhin, D. V.; Postnikova, T.Y.; Soboleva, E.B.; Zaitsev, A. V Short-Term Epileptiform Activity Potentiates Excitatory Synapses but Does Not Affect Intrinsic Membrane Properties of Pyramidal Neurons in the Rat Hippocampus In Vitro. *Biomedicines* **2021**, *9*, 1374, doi:10.3390/biomedicines9101374.
30. Rakhade, S.N.; Zhou, C.; Aujla, P.K.; Fishman, R.; Sucher, N.J.; Jensen, F.E. Early Alterations of AMPA Receptors Mediate Synaptic Potentiation Induced by Neonatal Seizures. *The Journal of Neuroscience* **2008**, *28*, 7979–7990, doi:10.1523/JNEUROSCI.1734-08.2008.
31. Joshi, S.; Rajasekaran, K.; Sun, H.; Williamson, J.; Kapur, J. Enhanced AMPA Receptor-Mediated Neurotransmission on CA1 Pyramidal Neurons during Status Epilepticus. *Neurobiol Dis* **2017**, *103*, 45–53, doi:10.1016/j.nbd.2017.03.017.
32. Owen, B.; Bichler, E.; Benveniste, M. Excitatory Synaptic Transmission in Hippocampal Area CA1 Is Enhanced Then Reduced as Chronic Epilepsy Progresses. *Neurobiol Dis* **2021**, *154*, 105343, doi:10.1016/j.nbd.2021.105343.
33. Clarkson, C.; Smeal, R.M.; Hasenoehrl, M.G.; White, J.A.; Rubio, M.E.; Wilcox, K.S. Ultrastructural and Functional Changes at the Tripartite Synapse during Epileptogenesis in a Model of Temporal Lobe Epilepsy. *Exp Neurol* **2020**, *326*, 113196, doi:10.1016/j.expneurol.2020.113196.
34. Amakhin, D. V.; Soboleva, E.B.; Ergina, J.L.; Malkin, S.L.; Chizhov, A. V.; Zaitsev, A. V. Seizure-Induced Potentiation of AMPA Receptor-Mediated Synaptic Transmission in the Entorhinal Cortex. *Front Cell Neurosci* **2018**, *12*, 486, doi:10.3389/fncel.2018.00486.
35. Malkin, S.L.; Amakhin, D. V.; Veniaminova, E.A.; Kim, K.K.; Zubareva, O.E.; Magazanik, L.G.; Zaitsev, A. V Changes of AMPA Receptor Properties in the Neocortex and Hippocampus Following Pilocarpine-Induced Status Epilepticus in Rats. *Neuroscience* **2016**, *327*, 146–155, doi:10.1016/j.neuroscience.2016.04.024.
36. Rajasekaran, K.; Todorovic, M.; Kapur, J. Calcium-Permeable AMPA Receptors Are Expressed in a Rodent Model of Status Epilepticus. *Ann Neurol* **2012**, *72*, 91–102, doi:10.1002/ana.23570.
37. Postnikova, T.Y.; Griflyuk, A. V.; Ergina, J.L.; Zubareva, O.E.; Zaitsev, A. V. Administration of Bacterial Lipopolysaccharide during Early Postnatal Ontogenesis Induces Transient Impairment of Long-Term Synaptic Plasticity Associated with Behavioral Abnormalities in Young Rats. *Pharmaceuticals* **2020**, *13*, 48, doi:10.3390/ph13030048.
38. Zubareva, O.E.; Postnikova, T.Y.; Grifluk, A. V.; Schwarz, A.P.; Smolensky, I. V.; Karepanov, A.A.; Vasilev, D.S.; Veniaminova, E.A.; Rotov, A.Y.; Kalemenev, S. V.; et al. Exposure to Bacterial Lipopolysaccharide in Early Life Affects the Expression of Ionotropic Glutamate Receptor Genes and Is Accompanied by Disturbances in Long-Term Potentiation and Cognitive Functions in Young Rats. *Brain Behav Immun* **2020**, *90*, 3–15, doi:10.1016/j.bbi.2020.07.034.
39. Mlynarik, M.; Johansson, B.B.; Jezova, D. Enriched Environment Influences Adrenocortical Response to Immune Challenge and Glutamate Receptor Gene Expression in Rat Hippocampus. *Ann N Y Acad Sci* **2004**, *1018*, 273–280, doi:10.1196/annals.1296.032.
40. Postnikova, T.Y.; Griflyuk, A.V.; Zhigulin, A.S.; Soboleva, E.B.; Barygin, O.I.; Amakhin, D.V.; Zaitsev, A.V. Febrile Seizures Cause a Rapid Depletion of Calcium-Permeable AMPA Receptors at the Synapses of Principal Neurons in the Entorhinal Cortex and Hippocampus of the Rat. *Int J Mol Sci* **2023**, *24*, doi:10.3390/ijms241612621.
41. Dubé, C.; Richichi, C.; Bender, R.A.; Chung, G.; Litt, B.; Baram, T.Z. Temporal Lobe Epilepsy after Experimental Prolonged Febrile Seizures: Prospective Analysis. *Brain* **2006**, *129*, 911–922, doi:10.1093/brain/awl018.
42. Gonzalez-Ramirez, M.; Salgado-Ceballos, H.; Orozco-Suarez, S.A.; Rocha, L. Hyperthermic Seizures and Hyperthermia in Immature Rats Modify the Subsequent Pentylentetrazole-Induced Seizures. *Seizure* **2009**, *18*, 533–536, doi:10.1016/j.seizure.2009.04.011.
43. Theodosis, D.T.; Poulain, D.A.; Oliek, S.H.R. Activity-Dependent Structural and Functional Plasticity of Astrocyte-Neuron Interactions. *Physiol Rev* **2008**, *88*, 983–1008, doi:10.1152/physrev.00036.2007.
44. Freeman, M.R. Specification and Morphogenesis of Astrocytes. *Science (1979)* **2010**, *330*, 774–778, doi:10.1126/science.1190928.

45. Griflyuk, A. V.; Postnikova, T.Y.; Zaitsev, A. V. Prolonged Febrile Seizures Impair Synaptic Plasticity and Alter Developmental Pattern of Glial Fibrillary Acidic Protein (GFAP)-Immunoreactive Astrocytes in the Hippocampus of Young Rats. *Int J Mol Sci* **2022**, *23*, 12224, doi:10.3390/ijms232012224.
46. Postnikova, T.Y.; Griflyuk, A. V.; Amakhin, D. V.; Kovalenko, A.A.; Soboleva, E.B.; Zubareva, O.E.; Zaitsev, A. V. Early Life Febrile Seizures Impair Hippocampal Synaptic Plasticity in Young Rats. *Int J Mol Sci* **2021**, *22*, 8218, doi:10.3390/ijms22158218.
47. Zhuravin, I.A.; Dubrovskaya, N.M.; Vasilev, D.S.; Postnikova, T.Y.; Zaitsev, A. V. Prenatal Hypoxia Produces Memory Deficits Associated with Impairment of Long-Term Synaptic Plasticity in Young Rats. *Neurobiol Learn Mem* **2019**, *164*, 107066, doi:10.1016/j.nlm.2019.107066.
48. Postnikova, T.Y.; Amakhin, D. V.; Trofimova, A.M.; Smolensky, I. V.; Zaitsev, A. V. Changes in Functional Properties of Rat Hippocampal Neurons Following Pentylentetrazole-Induced Status Epilepticus. *Neuroscience* **2019**, *399*, 103–116, doi:10.1016/j.neuroscience.2018.12.029.

Disclaimer/Publisher's Note: The statements, opinions and data contained in all publications are solely those of the individual author(s) and contributor(s) and not of MDPI and/or the editor(s). MDPI and/or the editor(s) disclaim responsibility for any injury to people or property resulting from any ideas, methods, instructions or products referred to in the content.